

Reversible heat pump HVAC system with regenerative heat exchanger for electric vehicles: analysis of its impact on driving range

Sara Bellocchi^a, Giuseppe Leo Guizzi^a, Michele Manno^{a,*}, Marco Salvatori^a,
Alessandro Zaccagnini^a

^a*Dept. of Industrial Engineering, University of Rome Tor Vergata, Italy*

Abstract

Besides providing energy for traction, an electric vehicle battery operates on-board auxiliary systems, among which air conditioning features the highest energy consumption and reduces significantly the driving range. Furthermore, electric vehicles heating needs are typically fulfilled through high-consuming resistors. In this respect, heat pumps promise higher energy efficiency and an increase in all-electric range.

This paper analyses a reversible heat pump HVAC system equipped with a regenerative heat exchanger for pre-conditioning and hygrometric comfort improvement, and assesses air-conditioning energy loads and their impact on driving range for a vehicle performing daily commutes in different Italian cities. The dynamic model was set up in a Modelica framework. The overall system integrates component models calibrated against experimental data.

Results confirm that air conditioning, consuming up to 32% of the energy required for traction on a daily commute, highly impacts on the all-electric range, which can decrease to 72 km from a base value of 94 km. In heating mode, replacing a resistor with a heat pump reduces consumption by 17–52% depending on geographical context, which proves to be highly effective in particularly demanding summer conditions lessening the driving range decrease up to 6%.

Keywords: Automotive air conditioning, HVAC, Electric vehicles, Regenerative heat exchanger, Heat pump

*Corresponding author

Email address: michele.manno@uniroma2.it (Michele Manno)

1 1. Introduction

2 Battery electric vehicles (EVs) are progressively emerging in the light-
3 duty passenger market, featuring a stock of 740 thousands in 2015, 60 times
4 more than in 2010 [1]. Remarkable efforts, under the joint support of gov-
5 ernments and industry, have been directed towards EVs as a promising al-
6 ternative to carbon intensive, polluting and oil dependent road transport.
7 However, despite offering low environmental impact and noise pollution along
8 with life-cycle cost savings and enhanced drivability, EVs large-scale adop-
9 tion and diffusion is still limited by comparatively higher purchase costs and
10 driving range restrictions [2–4].

11 On-board rechargeable batteries are the sole EVs power source, thus pro-
12 viding for both traction energy needs and auxiliary system requirements. Ve-
13 hicle heating, ventilation and air-conditioning system (HVAC) features the
14 highest energy consumption among all the accessory loads [5] and therefore
15 may consume a substantial amount of the total energy stored. This results
16 in a driving range reduction, further worsened by energy storage devices lim-
17 ited capacity. Previous studies have modeled the device-level function and
18 energy consumption of HVAC systems as well as the impact on the vehi-
19 cle driving range [6–11]. All these studies revealed a significant impact on
20 driving range; depending on air-conditioner size, driving cycle and external
21 weather conditions, the driving range decrease has been estimated in a range
22 between 16% and 36% [6]. This calls for maximizing the efficiency of climate
23 control systems to reduce energy consumption in both cooling and heating
24 modes. Advanced glazing, recirculated air and cabin pre-conditioning have
25 already been regarded as means of improving EVs conventional thermal con-
26 trol systems thus mitigating driving range reductions [6, 12, 13].

27 Moreover, thermal comfort loads feature significant variations depending
28 on external climate conditions. Thus, as the geographical context and time
29 of day change, so does the air conditioning load and the driving range in turn.
30 Although of key importance in affecting electric vehicles performance, previ-
31 ous studies estimated the air conditioning load disregarding hourly changes
32 in weather variables, using for instance a daily-mean radiant temperature to
33 describe a summer day for a given city [6] or two different temperatures for
34 summer and winter conditions [14]. Only few studies assessed the dynamic
35 variation of thermal loads as a function of location, season and time of the

36 day to ultimately quantify the effect of geographical and temporal differences
37 on the all-electric range [13, 15].

38 In particular, Kambly & Bradley have carried out a research work aiming
39 to quantitatively assess the extent to which the EV range is affected by cabin
40 comfort conditioning loads and therefore by external weather conditions [13,
41 15]. EV range is shown to vary widely across the geography of the US
42 throughout the time of day from a minimum of 95 km (for midday trips
43 in hot and sunny ambient conditions) to a maximum of 128 km (for early
44 morning trips in moderate ambient conditions). Commutes performed during
45 the middle portion of the day, where temperatures and solar radiation are at
46 their maximum values, feature the highest EV range reduction. Nevertheless,
47 in this study the heating needs are fulfilled by means of a relatively inefficient
48 resistance heater.

49 This solution is still typically adopted in EVs because of the lack of engine
50 waste heat to recycle [16, 17]. In particular, positive temperature coefficient
51 (PTC) heaters are widely used by the industry in EV cabin heating in place of
52 the engine coolant heater core of conventional vehicles [18–21]; however, these
53 systems present limitations related to high costs and energy consumption [22].

54 However, in EVs climate control systems, heat pumps seem a more sus-
55 tainable and efficient solution, so that heat pump (HP) systems are currently
56 stepping into EVs market [23–25] as a reasonable solution. Several studies
57 have been published demonstrating the feasibility of a reversible heat pump
58 system for electric vehicle air conditioning, pointing to Coefficients of Perfor-
59 mance (COP) slightly higher than 2 in heating mode and to electric driving
60 range improvement over the use of PTC by 5–10% at low and mid ambient
61 temperatures [26–33]. However, the dynamic performance of reversible heat
62 pump systems with reference to hourly distributions of climate variables,
63 geographical location and season has not been thoroughly evaluated in the
64 literature, except for Neubauer & Wood [32] who compared, among other
65 things, heat pump systems to conventional PTC heaters.

66 In this paper, the impact of geographical context, season and time of
67 day on cabin air conditioning energy needs is estimated for an electric vehi-
68 cle commuting in different Italian cities. The HVAC system is based on a
69 reversible heat pump, also equipped with a regenerative heat exchanger to
70 further improve efficiency and hygrometric conditions both in cooling and
71 heating operating modes. The performance of the proposed heat pump sys-
72 tem is compared to that of a conventional PTC resistor to assess the cor-
73 responding energy savings in heating mode. The energy consumed for air

74 conditioning and the resulting driving range reduction is dynamically eval-
75 uated for different commuting time options and locations throughout the
76 year.

77 The model of the HVAC system is implemented in Dymola (Dynamic
78 Modeling Laboratory), which provides a dynamic simulation environment
79 to accurately model integrated and complex systems [34]. In particular,
80 components from the Modelon Air Condition library [35] have been used
81 and customized to build up the overall system model. Each component has
82 been validated against experimental data provided by the original equipment
83 manufacturer.

84 Results establish to what extent climatic variables, geographical location
85 and time of travel affect the EV range, confirming that HVAC loads must
86 necessarily be taken into account when estimating the actual driving range.
87 The effectiveness of using a heat pump in place of PTC resistors and of the
88 regenerative heat exchanger in improving both EV range and cabin comfort
89 conditions has been assessed, evaluating under which climate conditions these
90 systems prove to significantly increase the overall energy efficiency.

91 2. Description of the HVAC system

92 In this section the reversible heat pump system used in the model will be
93 described. Reversible heat pump air conditioning systems work in A/C mode
94 for cabin cooling and in heat pump mode for cabin heating, by means of a 4-
95 way valve that allows to reverse the refrigerant cycle. Figs. 1 and 2 represent
96 the system schematic in cooling and heating mode respectively. A regener-
97 ative heat exchanger (ERV) has been also inserted for air preconditioning
98 purposes.

99 2.1. A/C operation

100 2.1.1. Air side

101 In cooling mode, outside air needs to be dehumidified and cooled down
102 to achieve cabin thermal comfort conditions. This is achieved through sub-
103 sequent conditioning processes as following:

- 104 1. The proposed system inserts an Energy Recovery Ventilator (ERV),
105 which is an air-to-air regenerative heat exchanger that allows the out-
106 side air flow to exchange both latent and sensible heat with air flowing
107 from the cabin by means of a separating membrane. The incoming air

- 108 mixture, interacting thermally with the recirculating flow, undergoes a
109 pre-cooling and dehumidification process, before entering the internal
110 heat exchanger, which acts as an evaporator in heating mode.
- 111 2. The air flows to the evaporator where it is further cooled down by
112 exchanging heat with the refrigerant.
 - 113 3. In mid-season cooling operation, the air exiting the evaporator may
114 reach unacceptable low values (below 3 °C) and some reheating may be
115 required before entering the cabin. In fact, despite working at the min-
116 imum speed, the compressor may still supply an excessive power when
117 ambient temperature values are relatively cool (but not cold enough
118 to provide for free cooling). Air reheating is achieved by means of an
119 auxiliary internal heat exchanger that acts a condenser.
 - 120 4. Having completed all the necessary conditioning treatments, air is ul-
121 timately blown into the cabin.

122 *2.1.2. Refrigerant side*

123 In cooling mode, the cabin thermal control system operates on a conven-
124 tional vapor-compression refrigerating cycle. The internal heat exchanger
125 acts as an evaporator in cooling mode, with the refrigerant absorbing heat
126 from the air exiting the ERV. If the air exiting the evaporator needs to be re-
127 heated, the required refrigerant flow will be directed toward a heater, which,
128 in turn, acts as a condenser allowing the working fluid to transfer heat to air
129 entering the cabin. The external heat exchanger, located close to the electric
130 motor and relatively far from the cabin, acts as a condenser in cooling mode,
131 allowing the refrigerant to change its state by means of a thermal interaction
132 with the outside air.

133 *2.2. Heating operation*

134 *2.2.1. Air side*

135 In heating mode (fig. 2), outside air needs to be humidified and heated
136 up to meet cabin thermal comfort requirements. This is achieved through
137 subsequent conditioning processes:

- 138 1. Fresh air from outside the vehicle goes to the ERV where it undergoes
139 a pre-heating and humidification process exchanging with air flowing
140 from the cabin, before entering the internal heat exchanger (condenser
141 in heating mode).

- 142 2. The air flows to the condenser where it is further heated up, exchanging
143 heat with the refrigerant.
- 144 3. The air exiting the condenser undergoes a reheating process passing
145 through the auxiliary condenser.
- 146 4. Having completed all the necessary conditioning treatments, air is ul-
147 timately blown into the cabin.

148 *2.2.2. Refrigerant side*

149 In heating mode, the cabin thermal control system operates on a heat
150 pump continuous cycle so as to heat the incoming outside air up to comfort
151 conditions. The refrigerant undergoes the same processes as those previously
152 described for the refrigerating cycle, differing however in the roles of the
153 internal and external heat exchangers. The internal heat exchanger now acts
154 as a condenser, allowing heat to be transferred from the refrigerant to the air
155 exiting the ERV. The external heat exchanger works instead as an evaporator,
156 allowing the refrigerant to change its state by means of a thermal interaction
157 with the outside air. The refrigerant flow is controlled by means of two four-
158 way valves, as illustrated in Figs. 1 and 2 (the valves are located next to the
159 compressor and the expansion valve), which allow to switch between cooling
160 and heating mode.

161 **3. Numerical model description**

162 *3.1. HVAC components*

163 The proposed system has been modeled and simulated in a Modelica/
164 Dymola framework. The model has been calibrated with reference to stan-
165 dard industry components, using Modelon Air Conditioning library features
166 [35].

167 *3.1.1. Media*

168 Modelon Air Conditioning library provides specific components to model
169 the fluids involved in the physical processes: refrigerant and outside air.

170 The refrigerant fluid undergoing the thermodynamic cycle is R134a. The
171 choice of not taking into account any possible replacement for this fluid,
172 despite the ban gradually introduced by European Union's f-gas regulations
173 (Regulation (EC) No 842/2006 and Directive 2006/40/EC), is justified by the
174 necessity to compare the results obtained with existing literature and exper-
175 imental data for model validation. Besides, under similar cooling capacity,

176 it has been demonstrated that the COPs of HVAC systems using R134a or
177 R1234yf as working fluids are comparable [36, 37].

178 The refrigerant R134a is modeled with reference to Helmholtz equation
179 from Span [38] and valid within a specific range of temperature and pressure,
180 precisely going from $-103\text{ }^{\circ}\text{C}$ to $102\text{ }^{\circ}\text{C}$ and 0.39 kPa to 70 MPa.

181 Air has been represented by means of the Modelon humid air model,
182 valid within 0 to $150\text{ }^{\circ}\text{C}$. Sources and sinks components are available in the
183 library to allow specific fluid parameters to be controlled. As for the air
184 entering the system, flow rate, temperature and relative humidity have been
185 set. Air temperature and relative humidity reflect the actual external weather
186 conditions throughout the year, made available by the Meteorological Service
187 of Aeronautica Militare [39] for different Italian cities.

188 3.1.2. Compressor

189 Electrically-driven compressors are typically employed in EV cabin ther-
190 mal control systems in place of mechanical compressors. These components
191 are directly powered by a brushless electric motor controlled by an inverter
192 to allow variable speed operations [40, 41]. In the proposed model, a MAS-
193 TERFLUX Sierra03-0982Y3 compressor [42] has been used as a reference in
194 terms of operating parameters and efficiencies.

195 The compressor has been modeled using the fixed displacement compo-
196 nent available in Modelon Air Conditioning library, which requires, as input
197 parameters, the compressor effective volumetric and isentropic efficiency.

198 Compressor performance depends on pressure ratio, compressor speed
199 and relative displacement. The minimum and maximum rotational speed
200 have been set respectively to 1800 and 6500 rpm. Compressor efficiencies
201 are defined via three tables that use pressure ratio and rotational speed
202 as inputs. Operating performance has been assessed with reference to the
203 Masterflux data sheet for a 48 V compressor [42]. The polynomial function
204 therein suggested has been used to estimate flow rate and power consumption,
205 evaluated as function of compressor speed and refrigerant temperature at the
206 suction and discharge sides.

207 3.1.3. Evaporator

208 In cooling mode, the internal heat exchanger, physically located by the
209 nozzles through which air enters the cabin, acts as an evaporator thus ensur-
210 ing the refrigerant change of state from liquid to slightly superheated vapor.
211 In heating mode, instead, it is the external heat exchanger, located in the

212 electric motor proximity and relatively far from the passenger cabin, that
213 acts as an evaporator.

214 The evaporator is a flat plate type and has been modeled in Dymola
215 using the available plate evaporator component provided in the Air Condi-
216 tioning library. This model for a compact automotive evaporator is based
217 on a microtube heat exchanger type for vertical refrigerant flow, which in
218 general allows heat transfer and refrigerant flow to change their direction.
219 The component provides accurate equations to model heat exchange [43, 44]
220 and pressure drops [45, 46].

221 3.1.4. Condenser

222 In heating mode, the internal heat exchanger located in the proximity
223 of the nozzles acts a condenser thus ensuring the refrigerant change of state
224 from superheated vapor to liquid. In cooling mode, instead, it is the external
225 heat exchanger that acts as a condenser. The condenser is a horizontal micro-
226 tubes type and has been modeled in Dymola using the condenser component
227 available in the Air Conditioning library.

228 The same equations as in the evaporator component are used to model
229 heat exchange and pressure drops.

230 3.1.5. Expansion Valve

231 The thermostatic expansion valve ensures the refrigerant to undergo a
232 pressure drop through an isenthalpic expansion process. An electronically-
233 regulated orifice controls the refrigerant flow rate by means of a temperature
234 sensor, ensuring the desired superheat temperature difference at the com-
235 pressor suction side [47].

236 3.1.6. Energy Recovery Ventilator (ERV)

237 Energy Recovery Ventilators are typically used in building air condi-
238 tioning systems for thermal comfort control [48, 49], but these components
239 are progressively being evaluated for application in the automotive industry
240 [50, 51].

241 In the proposed system, the ERV is based on two polymeric membranes,
242 which allow both latent and sensible heat exchange between the two circu-
243 lating fluids. Heat and mass (in the form of water molecules) are transferred,
244 while the passage of other molecules (such as carbon dioxide) is inhibited.
245 Contrary to a conventional heat exchanger, ERV selectivity allows the latent

246 heat to be transferred thus achieving potential advantages in terms of energy
247 savings related to air conditioning processes.

248 Outside air goes into the ERV where it interacts with air flowing from
249 the cabin. Latent and sensible heat are exchanged through the selective
250 membrane, resulting in an overall enhancement of air conditions.

251 A model of ERV has been created and implemented in Modelica with
252 reference to a $45 \times 20 \times 30$ cm industrial component [52], not specifically
253 developed for an automotive application. The amount of space taken could
254 be substantially reduced by decreasing the width of air flow passage, at the
255 price of a slight increase in pressure drops. Latent and sensible heat exchange
256 efficiency can be described as follows:

$$\eta_s = \frac{T_{out}^{(1)} - T_{in}^{(1)}}{T_{out}^{(2)} - T_{in}^{(1)}} \quad (1)$$

$$\eta_l = \frac{\omega_{out}^{(1)} - \omega_{in}^{(1)}}{\omega_{out}^{(2)} - \omega_{in}^{(1)}} \quad (2)$$

257 where:

- 258 • $T_{in}^{(1)}$, $\omega_{in}^{(1)}$, $T_{out}^{(1)}$ and $\omega_{out}^{(1)}$ are temperature and absolute humidity of out-
259 side air entering and exiting the ERV;
- 260 • $T_{out}^{(2)}$ and $\omega_{out}^{(2)}$ are temperature and absolute humidity of the cabin air
261 flow exiting the ERV.

262 ERV efficiencies (as shown in Fig. 3) were provided by the manufacturer
263 [52] as functions of air flow rate and implemented in the model to characterize
264 precisely the heat exchanger performance.

265 3.1.7. Model validation

266 The proposed air-conditioning system has been modeled using Mode-
267 lon Air Conditioning library, which features state-of-the-art air-conditioning
268 models specifically created with reference to automotive applications. This
269 library is a proven tool for air conditioning system design and virtual pro-
270 totyping in the automotive sector, as demonstrated by its wide adoption in
271 design, analysis and optimization of on-board air conditioning systems [5, 35].

272 Furthermore, the library provides several ways to calibrate and validate
273 design options and component settings. In this study, each component used

274 to model the HP system has been validated with reference to experimental
275 data provided by the equipment manufacturer: FIAT research center in the
276 case of heat exchangers (evaporator, condenser, heater core), and the com-
277 panies already mentioned in the corresponding preceding sections in the case
278 of compressor and ERV.

279 The accuracy of the model has thus been ensured by means of validation
280 against experimental data. By way of example, Fig. 4 reports the condenser
281 heat flux as a function of air flow rate over the entire operating range, showing
282 a good fit between model and available data, with a maximum discrepancy of
283 6%, well within the acceptable range and the experimental data uncertainty.

284 3.2. Thermal loads

285 Heating and cooling thermal loads are essential to assess HVAC power
286 requirements and energy consumption and consist of the following contribu-
287 tions:

- 288 • radiation load;
- 289 • environmental load;
- 290 • metabolic load;
- 291 • ventilation load.

292 A specific component has been created in Modelica to model thermal
293 loads within the cabin as function of geographical location and time of travel
294 by implementing the necessary heat exchange and heat balance equations
295 [53].

296 3.2.1. Radiation load

297 The thermal load due to the effect of solar radiation can be divided into
298 direct and diffuse components, leading to the following fluxes:

$$\dot{Q}_{dir} = \sum_{surfaces} S\dot{I}_{dir} \cos \zeta \quad (3)$$

$$\dot{Q}_{dif} = \sum_{surfaces} S\dot{I}_{dif} \quad (4)$$

299 where S is the surface considered, I_{dir} and I_{dif} are respectively the direct and
300 diffuse radiation acting on the surface and ζ is the angle between sun's rays
301 and the line normal to the surface.

302 The amount of incident solar power depends on a number of factors:

- 303 • solar radiation geometry, which is based on solar angles, evaluated as
304 function of location/latitude, season/time of year and time of day;
- 305 • local climate variables;
- 306 • inclination of the collecting surface in the direction of the sun.

307 The amount of solar energy is thus highly affected by the particular geo-
308 graphical context, time of travel and relative geometry between vehicle sur-
309 faces and sun rays. In order to estimate accurately energy requirements for
310 cabin comfort needs, a dynamic variation of climatic variables during the
311 day and throughout the year has been implemented in the model. Dry bulb
312 temperature and relative humidity values have been made available by the
313 Meteorological Service of Aeronautica Militare [39] for different Italian cities
314 and, for each month of the year, an average daily trend has been estimated.

315 Figs. 5 and 6 represent Rome average days in terms of air temperature
316 (5a, 6a) and relative humidity (5b, 6b) for winter and summer months re-
317 spectively. This procedure has been repeated for climate data belonging to
318 different Italian cities, specifically Rome, Turin, Milan, Bologna, Bari and
319 Naples. Temperature and relative humidity are compared in Figs. 7 and 8
320 for the different cities analyzed with regard to a typical winter and summer
321 month daily trend.

322 According to the Mediterranean Italian climate, cabin heating might be
323 required in some spring days and cooling might still be necessary in the
324 beginning of autumn, generally during seasonal transition periods. Hence,
325 April and October have been included in both summer and winter months
326 potentially entailing the cabin control system to work either in heating or
327 cooling mode depending on the particular weather conditions.

328 The relative inclination between vehicle surfaces and sun's rays has been
329 randomized and the latitude varied according to the city analyzed.

330 Given that the amount of direct radiation varies depending on cloudiness,
331 for each month of the year the number of overcast and sunny days has been
332 taken into account. The radiation load representative of the average day has
333 been derived as a weighted average between these two conditions over the
334 entire month.

335 *3.2.2. Ambient load*

336 Environmental conditions highly affect the thermal load acting on the
337 vehicle. The heat flux exchanged between vehicle and environment can be
338 expressed as:

$$\dot{Q}_{amb} = \sum_{surfaces} SU(T_{amb} - T_{int}) \quad (5)$$

339 where the global heat exchange coefficient includes convection and conduc-
340 tion heat transfer coefficients:

$$U = \left(\frac{1}{h_e} + \frac{\lambda}{k} + \frac{1}{h_i} \right)^{-1} \quad (6)$$

341 In particular, the external convective heat transfer coefficient h_e has
342 been empirically modeled and calibrated with reference to cabin tempera-
343 ture as provided in [13]. This results in the following relation, where h_e is in
344 $W/(m^2 K)$ and v in m/s :

$$h_e = 8.68 + 6.64\sqrt{v} \quad (7)$$

345 *3.2.3. Metabolic load*

346 Passengers and driver metabolism generates a thermal load quantifiable
347 as a function of the number of occupants, their height and weight, including
348 a coefficient representing their metabolic activity, as follows [53]:

$$\dot{Q}_{met} = \sum_{passengers} MA_{body} \quad (8)$$

349 where M is a metabolic factor equal to $85 W/m^2$ and $55 W/m^2$ for driver and
350 passengers respectively, while A_{body} is an estimate value for the body surface
351 dependent on passengers height and weight.

352 In the proposed model, the cabin is occupied by the driver only; the
353 passengers metabolic loads are disregarded as a result.

354 *3.2.4. Ventilation load*

355 Fresh air requirements within a cabin recommend a certain air change rate
356 to keep carbon dioxide level, generated by passengers' metabolism, under a
357 certain level [54]. The corresponding heat flux can be expressed as follows:

$$\dot{Q}_{vent} = \dot{m}_{vent}(h_{ext} - h_{int}) \quad (9)$$

358 *3.3. Vehicle cabin*

359 The cabin has been characterized in terms of geometry and physical prop-
360 erties separately for each surface making up the cabin: windows, doors, roof,
361 floor, boot, firewall and windscreen. Data refer to the FIAT Panda model
362 and have been provided by FIAT Research Center.

363 *3.3.1. Geometry*

364 The vehicle cabin has been modeled with reference to a generic light-duty
365 passenger car features. The different surfaces making up the vehicle exte-
366 rior have been modeled considering their relative inclination and area thus
367 allowing a reliable and accurate estimation of radiation and environmental
368 loads.

369 *3.3.2. Physical properties*

370 Surfaces physical properties have been included in the thermal model in
371 terms of absorption, transmissivity, convection and conduction coefficients
372 and thickness.

373 *3.3.3. Cabin validation*

374 The cabin behavior has been verified by running the model assuming the
375 vehicle parked outdoor and subject to the radiation load with the HVAC
376 turned off, and comparing the obtained internal temperature values with
377 results available in literature. In particular, the system has been simulated
378 under the same climate conditions as those used by Kambly & Bradley [13],
379 and the comparable response in terms of interior temperature daily profile
380 proves the model validity.

381 *3.4. Driving cycle*

382 The driving cycle selected for the analysis is the Worldwide harmonized
383 Light vehicles Test Cycle (WLTC) implemented in the first global standard
384 procedure for determining the levels of pollutants and CO₂ emissions, fuel
385 or energy consumption, and electric range from light-duty vehicles [55]. The
386 cycle total distance is 23.26 km featuring a duration of 1800 s and an average
387 speed equal to 46.5 km/h. The cycle is made up of four speed zones: one rep-
388 resentative of urban driving, one suburban driving, one extra-urban driving,
389 and a highway zone.

390 The driving cycle well represents the average distance for daily commutes
391 in Italy for people who have to partially drive on highway to get to work [56];
392 in fact, if repeated twice per day, it covers a total distance of 46.52 km.

393 For a typical light-duty passenger vehicle, the electric energy required to
394 perform a WLTC cycle has been estimated as approximately 17 kWh/100km
395 [57], in line with other values reported in literature [14, 58–60]. With ref-
396 erence to a battery capacity of 16 kWh [61], the resulting driving range will
397 be equal to 94 km, if only energy for traction is taken into account and the
398 battery fully discharged. However, range values can significantly decrease
399 when HVAC consumption is considered.

400 4. Results and discussion

401 4.1. Model setup

402 The model assesses the cabin thermal comfort energy demand as a func-
403 tion of day and time of the year, for a vehicle performing daily commutes in
404 different Italian cities. Fig. 9 represents a schematic of the model including
405 the system components as previously described.

406 The simulation requires the following input variables that can be cho-
407 sen at user's will to represent a particular geographical context and vehicle
408 utilisation mode:

- 409 ● day and month of the year;
- 410 ● duration of travel;
- 411 ● driving cycle;
- 412 ● trip start time;
- 413 ● city, characterised in terms of:
 - 414 – outside temperature;
 - 415 – outside relative humidity;
 - 416 – latitude.

417 The model provides results in terms of HVAC performance: it monitors
418 and controls temperature, and calculates the electric power consumption by
419 the compressor and HVAC auxiliary components such as fans, the overall

420 COP, and so on. A PID controller is employed to regulate the compressor
421 speed so as to maintain cabin comfort conditions, specifically set to 22 and
422 24 °C respectively in heating and cooling mode.

423 In order to estimate potential ERV savings with respect to traditional
424 heat-pump HVAC systems, two other similar models have been also imple-
425 mented in Dymola, representing respectively:

- 426 • a heat-pump HVAC system without air recirculation and ERV. This
427 model will be identified as the *base* case scenario, where air is contin-
428 ually drawn into the internal heat exchanger from the outside without
429 being preprocessed;
- 430 • a heat-pump HVAC system with air recirculation and without ERV.
431 This model entails a fixed air flow from the outside equal to 0.04 kg/s as
432 to guarantee sufficient air renewal (for 4 passengers approximately) and
433 a remaining recirculating air flow varying depending on power require-
434 ments. As a result, the recirculating air flow ranges from a minimum
435 of 0 to a maximum of 60% of the total air flow rate.

436 Models have been first tested with reference to Rome average climatic
437 conditions; results have been analysed and compared for the above-mentioned
438 different case scenarios.

439 *4.2. Seasonal and temporal effects on HVAC energy consumption*

440 Testing the basic HVAC system model (i.e. without air recirculation and
441 ERV) on the most demanding condition (i.e. July at 13:00), a displacement of
442 35 cm³ proves to be adequate to fulfill thermal comfort requirements. How-
443 ever, the adoption of an ERV or a recirculation system allows to achieve cabin
444 thermal comfort by employing a significantly smaller compressor (24 cm³).

445 The energy required for cabin cooling and heating has been estimated
446 and shown in Figs. 10 and 11 by simulating a basic heat-pump HVAC sys-
447 tem model without air recirculation and ERV. The energy required for HVAC
448 is divided into compressor and ventilation consumption, expressed as a per-
449 centage of the energy for traction and evaluated for three different times of
450 travel, i.e. 8:00, 13:00, 18:00, and month of the year.

451 In summertime, commuting performed during midday hours feature the
452 highest energy consumption, with a peak of 38%, with a significant increase
453 in July and August as compared to the other summer months. Travels per-
454 formed at 8:00 and 18:00 show comparable values in terms of HVAC energy

455 requirements which are always below 30% of the energy required for traction
456 and slightly higher for evening commuting. HVAC energy can be neglected
457 for April regardless of the time of travel.

458 As for winter months, the highest amount of energy for cabin thermal
459 control is required at 8:00, although evening travels are comparable in terms
460 of energy consumption. Precisely, the most demanding months are January,
461 February and December requiring approximately 16% of traction energy for
462 cabin heating. HVAC energy can be neglected for April regardless of the
463 time of travel being lower than 3% in any case.

464 Overall, the energy required for air conditioning represents a significant
465 load to be fulfilled, featuring a significant variation during the day and the
466 year depending on external weather conditions. Particularly, on average it
467 ranges from 5% to 35% in summer and from 3% to 16% in winter. Summer
468 loads may be more than twice than winter ones when peak conditions are
469 compared (i.e. December in winter and July in summer). Season transition
470 periods (i.e. April and October) show the smallest energy loads for cabin
471 thermal control; in fact, most of the time free heating or cooling proves to
472 be enough to cater for HVAC needs. Fan consumption is always a negligible
473 percentage of the total HVAC energy.

474 4.3. ERV performance

475 HVAC energy consumption has been assessed for each model and Fig. 12
476 compares compressor electric power requirements for the three simulated
477 scenarios (i.e. base, air recirculation and ERV) for a travel performed in
478 July at 13:00.

479 For HVAC systems employing an ERV or an air recirculation system,
480 power consumption is significantly lower than the base case on summer peak
481 conditions. This results in an energy reduction to achieve thermal com-
482 fort needs and, therefore, in an increased driving range. In this respect,
483 Fig. 13 displays the ratio E_{HVAC}/E_{trac} and the driving range with reference
484 to the theoretical range when HVAC consumption is not taken into account,
485 i.e. 94 km, over the entire day for the three models.

486 Pre-cooling through either the regenerative heat exchanger and the air
487 recirculation brings about similar advantages in terms of HVAC energy con-
488 sumption allowing a reduction of up to 14% of HVAC energy expressed as
489 a percentage of the energy required for traction, with corresponding bene-
490 fits on the driving range. However, an ERV-equipped HVAC system allows
491 additional advantages in terms of hygrometric comfort by regulating cabin

492 air humidity besides its temperature and guaranteeing a continuous supply
493 of fresh air. For this reason, an ERV system has been identified as the most
494 suitable solution to improve efficiency and comfort.

495 It is worth mentioning that both the ERV and the recirculation system
496 start operating only when the cabin temperature becomes lower than outside
497 temperature, thus the initial transient period to bring the cabin temperature
498 to comfort levels is automatically excluded. This results in both ERV and
499 recirculation functioning only for 60% of the total travel time, that in our
500 simulation is 30 min. If the duration of the travel increased, pre-cooling/
501 recirculation benefits would increase in turn.

502 HVAC energy savings have been estimated for the same travel times as
503 above and shown in Fig. 14 only for the ERV model, given that both ERV
504 and air recirculation provide very similar results. The ERV proves to be
505 highly effective in particularly demanding weather conditions, i.e. July and
506 August at 13:00 travel time, saving up to 13% of the total energy required
507 for both traction and air-conditioning as compared to HVAC consumption
508 for the base case scenario. This results in a corresponding increase of the
509 driving range. However, when outside temperatures are relatively cooler, the
510 use of ERV does not bring about advantages in terms of energy savings, at
511 least for the Italian type of climate.

512 4.4. HVAC energy consumption: impact of geographical location

513 A similar analysis has been carried out for winter months and extended to
514 other Italian cities. Values of the ratio E_{HVAC}/E_{trac} and the resulting driving
515 range, for both summer and winter seasons, have been assessed considering
516 two different commutes with the outward travel occurring in both cases at
517 8:00 and two different return travel times respectively at 13:00 and 18:00.
518 Outward and return travels feature the same duration and follow the WLTC
519 driving cycle. Results are summarized in Figs. 15–18 in terms of seasonal
520 distribution of HVAC energy consumption and driving range for summer and
521 winter and for both commuting options. The boxplots show the minimum,
522 first quartile, median and mean, third quartile, and maximum values for
523 HVAC energy over the season analysed. Results are compared between the
524 base and the ERV-equipped HVAC system.

525 In summer, daily commutes including an evening travel are advantageous
526 in terms of HVAC energy consumption and obviously Southern Italy proves
527 to more affected by external weather conditions than the North. With ref-
528 erence to the base case scenario, this results in Bari featuring the highest

529 energy needs for cabin cooling, with a maximum of 32% of the energy for
530 traction and an average E_{HVAC}/E_{trac} equal to 15% and 12.5% for return trav-
531 els occurring respectively at 13:00 and 18:00. The driving range proves to
532 be highly affected by the air-conditioning energy needs and can be reduced
533 down to 72 km in the worst case. Turin here shows the lowest HVAC loads
534 with an average value of 10% and 8% of the energy required for traction for
535 return travels at 13:00 and 18:00. As compared to the base case, using an
536 ERV-equipped air-conditioning system, the driving range reduction can be
537 decreased up to approximately 6% and, on average, by 3%.

538 In winter, commutes including an evening return travel obviously require
539 higher HVAC energy loads than return travels at 13:00. Among the different
540 Italian cities analysed, Turin shows the highest HVAC energy consumption
541 with E_{HVAC}/E_{trac} a maximum of 20% and average values equal to 10% and
542 13% for return travels occurring respectively at 13:00 and 18:00 employing a
543 base HVAC system. As a consequence, the driving range can be reduced down
544 to 79 km. On the other hand, Naples features the lowest energy consumption
545 for cabin comfort needs, precisely 5 and 7.5% of the energy required for
546 traction for return travels at 13:00 and 18:00. Results reflect the difference in
547 weather variables between Northern and Southern Italy. An ERV-equipped
548 air-conditioning system allows to decrease the driving range reduction up to
549 approximately 4% and, on average, by 2%.

550 4.5. Estimate of HVAC annual energy consumption

551 Finally, the benefits of the adoption of an ERV-equipped system in terms
552 of energy savings over the entire year have been quantified considering 20
553 daily commutes per month. Results are summarized in Fig. 19.

554 HVAC energy requirements assessed over the entire year for the different
555 Italian cities reveal that the energy required for cabin thermal control is in the
556 range 200–250 kWh, i.e. 10–13% of traction energy. Moreover, the difference
557 between North and South Italy appears to be levelled out once the whole
558 year is taken into account. The adoption of a HVAC system employing a
559 regenerative heat exchanger reduces energy consumption by 20–25%.

560 In wintertime, the advantages of employing a heat pump-based system
561 over conventional PTC resistors can be quickly assessed through its COP.
562 Fig. 20 show average COP values in winter operating conditions. It is worth
563 mentioning that COP is penalized by relatively long transients compared
564 to the actual travel time of 30 min only. COP in winter ranges between
565 1.2 and 1.9 for a basic heat pump-based HVAC system and from 1.3 to 2.1

566 for an analogous system equipped with an ERV. The cabin thermal power
567 requirement being equal, this results in energy savings ranging between 17
568 and 52% when conventional PTC resistors are substituted with a heat pump-
569 based HVAC system.

570 5. Conclusions

571 This study assesses how location, season and time of the day affect HVAC
572 loads and driving range of an electric vehicle performing daily commutes
573 in different Italian cities. A reversible heat pump air-conditioning system
574 equipped with a regenerative heat exchanger (ERV) has been modeled and
575 the energy consumed for air conditioning purposes dynamically evaluated for
576 different commuting times and locations throughout the year. The outcomes
577 of this model have been compared with those of two other models representing
578 respectively a basic heat pump HVAC system and a heat pump HVAC system
579 employing a variable recirculating air flow.

580 Results confirm that cabin air-conditioning consumes a significant amount
581 of power and therefore must be taken into account when estimating the actual
582 driving range. HVAC loads have been assessed throughout the year for the
583 basic HVAC system in the first place, showing that energy consumed for EV
584 air-conditioning purposes can be as high as 38% of the energy required for
585 traction, highly affecting the driving range that can reduce from 94 km, when
586 air-conditioning loads are not taken into account, down to 68 km in the most
587 demanding summer conditions. Both time and location of commute affect
588 substantially the energy consumption.

589 The adoption of a regenerative heat exchanger proves to be effective from
590 an energy efficiency perspective, lessening the driving range reduction by 2–
591 6%, a figure that can increase with the duration of the travel. Therefore,
592 a heat pump-based HVAC system provided with an ERV allows significant
593 energy savings, comparable to what could be achieved with air recirculation,
594 along with a full cabin air renewal as an additional benefit, while taking a
595 reasonably small amount of space.

596 In heating mode, the average effectiveness of heat pump systems used in
597 place of PTC resistors for cabin heating brings about energy savings in the
598 range 17–52% depending on the geographical context and on the employment
599 of an ERV-equipped system.

600 Overall, HVAC energy requirements assessed over the entire year for the
601 different Italian cities reveal that the energy required for EVs thermal comfort

602 needs is in the range 200–250 kWh, i.e. 10–13% of traction energy, proving
603 to be a significant parameter to be considered when evaluating the actual
604 driving range of an electric vehicle.

605 Acknowledgements

606 This work was supported by the Italian Ministry for Development in
607 the framework of “Industria 2015 Bando Nuove Tecnologie per la mobilità
608 sostenibile”, project n. MS01_00011 “MECCANO”.

609 The authors would also like to acknowledge the invaluable effort provided
610 by all undergraduate students that worked on the project: Elisa Capuano,
611 Simone Noce, Francesco Sabatini and Leonardo Santaroni, as well as the
612 contribution of Meteorological Service of Aeronautica Militare, for having
613 provided climatic data.

614 References

- 615 [1] Cazzola P, Gorner M, Teter J, Yi W. Global EV Out-
616 look 2016. Tech. Rep.; International Energy Agency; 2016.
617 URL: [https://www.iea.org/publications/freepublications/
618 publication/global-ev-outlook-2016.html](https://www.iea.org/publications/freepublications/publication/global-ev-outlook-2016.html).
- 619 [2] Hawkins TR, Singh B, Majeau-Bettez G, Strømman AH. Comparative
620 Environmental Life Cycle Assessment of Conventional and Electric Ve-
621 hicles. *J Ind Ecol* 2013;17(1):53–64. doi:10.1111/j.1530-9290.2012.
622 00532.x.
- 623 [3] Michalek JJ, Chester M, Jaramillo P, Samaras C, Shiao CSN, Lave LB.
624 Valuation of plug-in vehicle life-cycle air emissions and oil displacement
625 benefits. *Proc Natl Acad Sci USA* 2011;108(40):16554–8. doi:10.1073/
626 pnas.1104473108.
- 627 [4] Duvall M. Advanced Batteries for Electric-Drive Vehicles A Tech-
628 nology and Cost-Effectiveness Assessment for Battery Electric Ve-
629 hicles, Power Assist Hybrid Electric Vehicles, and Plug-In Hy-
630 brid Electric Vehicles. Tech. Rep.; Electric Power Research
631 Institute; 2016. URL: [http://www.epri.com/abstracts/Pages/
632 ProductAbstract.aspx?ProductId=00000000001009299](http://www.epri.com/abstracts/Pages/ProductAbstract.aspx?ProductId=00000000001009299).

- 633 [5] Shojaei S, Robinson S, Chatham C, McGordon A, Marco J. Modelling
634 the Electric Air Conditioning System in a Commercially Available Ve-
635 hicle for Energy Management Optimisation. In: SAE Technical Paper.
636 SAE International; 2015,doi:10.4271/2015-01-0331.
- 637 [6] Farrington R, Rugh J. Impact of Vehicle Air-Conditioning on Fuel Econ-
638 omy, Tailpipe Emissions, and Electric Vehicle Range. Tech. Rep.; Na-
639 tional Renewable Energy Laboratory; 2000. URL: [http://www.nrel.
640 gov/docs/fy00osti/28960.pdf](http://www.nrel.gov/docs/fy00osti/28960.pdf).
- 641 [7] Hendricks TJ. Vehicle Transient Air Conditioning Analysis: Model
642 Development & System Optimization Investigations. Tech. Rep.; Na-
643 tional Renewable Energy Laboratory; 2001. URL: [http://www.nrel.
644 gov/docs/fy01osti/30715.pdf](http://www.nrel.gov/docs/fy01osti/30715.pdf).
- 645 [8] Rugh J. Integrated numerical modeling process for evaluating automo-
646 bile climate control systems. In: SAE Technical Paper. SAE Interna-
647 tional; 2002,doi:10.4271/2002-01-1956.
- 648 [9] Johnson VH. Fuel used for vehicle air conditioning: a state-by-state
649 thermal comfort-based approach. In: SAE Technical Paper. SAE Inter-
650 national; 2002,doi:10.4271/2002-01-1957.
- 651 [10] Torregrosa B, Payá J, Corberán J. Modelling of mobile air conditioning
652 systems for electric vehicles. In: 4th European Workshop on Mobile Air
653 Conditioning and Vehicle Thermal Systems. Turin; 2011,.
- 654 [11] Lee JT, Kwon S, Lim Y, Chon MS, Kim D. Effect of Air-Conditioning on
655 Driving Range of Electric Vehicle for Various Driving Modes. In: SAE
656 Technical Paper. SAE International; 2013,doi:10.4271/2013-01-0040.
- 657 [12] Barnitt RA, Brooker AD, Ramroth L, Rugh J, Smith KA. Analysis
658 of Off-Board Powered Thermal Preconditioning in Electric Drive Vehi-
659 cles. In: 25th World Batter. Hybrid Fuel Cell Electr. Shenzhen, China;
660 2010,URL: www.nrel.gov/docs/fy11osti/49252.pdf.
- 661 [13] Kambly K, Bradley TH. Geographical and temporal differences in elec-
662 tric vehicle range due to cabin conditioning energy consumption. J Power
663 Sources 2015;275:468–75. doi:10.1016/j.jpowsour.2014.10.142.

- 664 [14] Gennaro MD, Paffumi E, Martini G, Manfredi U, Scholz H, Lacher H,
665 et al. Experimental investigation of the energy efficiency of an electric
666 vehicle in different driving conditions. In: SAE Technical Paper. SAE
667 International; 2014,doi:[10.4271/2014-01-1817](https://doi.org/10.4271/2014-01-1817).
- 668 [15] Kambly KR, Bradley TH. Estimating the HVAC energy consumption
669 of plug-in electric vehicles. *Journal of Power Sources* 2014;259:117–24.
670 doi:[10.1016/j.jpowsour.2014.02.033](https://doi.org/10.1016/j.jpowsour.2014.02.033).
- 671 [16] Zhang J. Structural features of fully electric air conditioning system.
672 *Automob Maint* 2006;12:4–5.
- 673 [17] Guyonvarch G, Aloup C, Petitjean C, de Monts de Savasse A. 42V
674 Electric Air Conditioning Systems (E-A/CS) for Low Emissions, Archi-
675 tecture, Comfort and Safety of Next Generation Vehicles. SAE Technical
676 Paper 2001;doi:[10.4271/2001-01-2500](https://doi.org/10.4271/2001-01-2500).
- 677 [18] Umezu K, Noyama H. Air-Conditioning system For Electric Vehicles
678 (i-MiEV). In: SAE Automotive Alternate Refrigerant Systems Symposi-
679 um. 2010,URL: [http://www.sae.org/events/aars/presentations/
680 2010/W2.pdf](http://www.sae.org/events/aars/presentations/2010/W2.pdf).
- 681 [19] 2015 Smart Electric Drive Manual. 2014. URL: [https:
682 //www.smart.com/content/dam/smart/CA/pdf/2015_smart_
683 electric_drive_manual6522008013_FINAL.pdf](https://www.smart.com/content/dam/smart/CA/pdf/2015_smart_electric_drive_manual6522008013_FINAL.pdf).
- 684 [20] Life Cycle Environmental Certificate Mercedes-Benz B-Class Elec-
685 tric Drive. 2014. URL: [https://www.daimler.com/images/
686 sustainability/produkt/new-enviromentalcertificates/
687 daimler-umweltzertifikat-mb-b-klasse-electric-drive.pdf](https://www.daimler.com/images/sustainability/produkt/new-enviromentalcertificates/daimler-umweltzertifikat-mb-b-klasse-electric-drive.pdf).
- 688 [21] Meyer J. Advanced Climate Systems for EV Extended Range (ACS-
689 forEVER). In: DoE Vehicle Technologies Office Merit Review 2015.
690 Halla Visteon Climate Control Corp.; 2015,URL: [https://energy.gov/
691 sites/prod/files/2015/07/f24/vss135_meyer_2015_o.pdf](https://energy.gov/sites/prod/files/2015/07/f24/vss135_meyer_2015_o.pdf).
- 692 [22] Qi Z. Advances on air conditioning and heat pump system in electric
693 vehicles – A review. *Renew Sustain Energy Rev* 2014;38:754–64. doi:[10.
694 1016/j.rser.2014.07.038](https://doi.org/10.1016/j.rser.2014.07.038).

- 695 [23] Nissan LEAF Heat-Pump Cabin Heater. 2014. URL:
696 [http://www.nissan-global.com/EN/TECHNOLOGY/OVERVIEW/heat_](http://www.nissan-global.com/EN/TECHNOLOGY/OVERVIEW/heat_pump_cabin_heater.html)
697 [pump_cabin_heater.html](http://www.nissan-global.com/EN/TECHNOLOGY/OVERVIEW/heat_pump_cabin_heater.html).
- 698 [24] The e-Golf Product Guide. 2016. URL: [http://www.volkswagen.](http://www.volkswagen.ie/content/medialib/vwd4/ie/pdf-downloads/product-guides/e-golf-product-guide/_jcr_content/renditions/rendition.download_attachment.file/161005_ek_e-golf_october-2016.pdf)
699 [ie/content/medialib/vwd4/ie/pdf-downloads/product-guides/](http://www.volkswagen.ie/content/medialib/vwd4/ie/pdf-downloads/product-guides/e-golf-product-guide/_jcr_content/renditions/rendition.download_attachment.file/161005_ek_e-golf_october-2016.pdf)
700 [e-golf-product-guide/_jcr_content/renditions/rendition.](http://www.volkswagen.ie/content/medialib/vwd4/ie/pdf-downloads/product-guides/e-golf-product-guide/_jcr_content/renditions/rendition.download_attachment.file/161005_ek_e-golf_october-2016.pdf)
701 [download_attachment.file/161005_ek_e-golf_october-2016.pdf](http://www.volkswagen.ie/content/medialib/vwd4/ie/pdf-downloads/product-guides/e-golf-product-guide/_jcr_content/renditions/rendition.download_attachment.file/161005_ek_e-golf_october-2016.pdf).
- 702 [25] The heat pump or how to optimize Zoe's range. 2015.
703 URL: [https://group.renault.com/en/passion-2/innovation/](https://group.renault.com/en/passion-2/innovation/renault-a-born-innovator/heat-pump/)
704 [renault-a-born-innovator/heat-pump/](https://group.renault.com/en/passion-2/innovation/renault-a-born-innovator/heat-pump/).
- 705 [26] Suzuki T, Ishii K. Air Conditioning System for Electric Vehicle. In:
706 SAE Technical Paper. SAE International; 1996,doi:10.4271/960688.
- 707 [27] Meyer J, Yang G, Papoulis E. R134a Heat Pump for Improved Passenger
708 Comfort 2004;doi:10.4271/2004-01-1379.
- 709 [28] Pommé V. Reversible Heat Pump System for an Electrical Vehicle. In:
710 SAE Technical Paper. SAE International; 1997,doi:10.4271/971772.
- 711 [29] Kowsky C, Wolfe E, Leitzel L, Oddi F. Unitary HPAC System. SAE
712 Int J Passeng Cars - Mech Syst 2012;5(2):1016–25. doi:10.4271/
713 [2012-01-1050](https://doi.org/10.4271/2012-01-1050).
- 714 [30] Hosoz M, Direk M. Performance evaluation of an integrated automotive
715 air conditioning and heat pump system. Energy Conversion and Man-
716 agement 2006;47(5):545–59. doi:10.1016/j.enconman.2005.05.004.
- 717 [31] Yokoyama A, Osaka T, Imanishi Y, Sekiya S. Thermal management
718 system for electric vehicles. SAE Int J Mater Manuf 2011;4:1277–85.
719 doi:10.4271/2011-01-1336.
- 720 [32] Neubauer J, Wood E. Thru-life impacts of driver aggression, climate,
721 cabin thermal management, and battery thermal management on bat-
722 tery electric vehicle utility. Journal of Power Sources 2014;259:262–75.
723 doi:10.1016/j.jpowsour.2014.02.083.
- 724 [33] Hosoz M, Direk M, Yigit KS, Canakci M, Turkcan A, Alptekin E, et al.
725 Performance evaluation of an R134a automotive heat pump system for

- 726 various heat sources in comparison with baseline heating system. Appl
727 Therm Eng 2015;78:419–27. doi:10.1016/j.applthermaleng.2014.
728 12.072.
- 729 [34] DYMOLA Systems Engineering. Last retrieved on June 2017.
730 URL: [https://www.3ds.com/products-services/catia/products/
731 dymola](https://www.3ds.com/products-services/catia/products/dymola).
- 732 [35] Air Conditioning Library, User Guide. Last retrieved on March 2017.
733 URL: [http://www.modelon.com/products/modelica-libraries/
734 air-conditioning-library/](http://www.modelon.com/products/modelica-libraries/air-conditioning-library/).
- 735 [36] Daviran S, Kasaeian A, Golzari S, Mahian O, Nasirivatan S, Wongwises
736 S. A comparative study on the performance of HFO-1234yf and HFC-
737 134a as an alternative in automotive air conditioning systems. Appl
738 Therm Eng 2017;110:1091–100. doi:10.1016/j.applthermaleng.2016.
739 09.034.
- 740 [37] Lee Y, Jung D. A brief performance comparison of R1234yf and R134a
741 in a bench tester for automobile applications. Applied Thermal Engi-
742 neering 2012;35:240–2. doi:10.1016/j.applthermaleng.2011.09.004.
- 743 [38] Span R, Wagner W. Equations of State for Technical Applications.
744 III. Results for Polar Fluids. International Journal of Thermophysics
745 2003;24(1):111–62. doi:10.1023/A:1022362231796.
- 746 [39] Servizio Meteorologico Aeronautica Militare. 2014. URL: [http://www.
747 meteoam.it/](http://www.meteoam.it/).
- 748 [40] Cho H, Park C. Experimental investigation of performance and ex-
749 ergy analysis of automotive air conditioning systems using refrigerant
750 R1234yf at various compressor speeds. Appl Therm Eng 2016;101:30–7.
751 doi:10.1016/j.applthermaleng.2016.01.153.
- 752 [41] Tian Z, Qian C, Gu B, Yang L, Liu F. Electric vehicle air condition-
753 ing system performance prediction based on artificial neural network.
754 Appl Therm Eng 2015;89:101–14. doi:10.1016/j.applthermaleng.
755 2015.06.002.
- 756 [42] SIERRA03-0982Y3 - Data Sheet. 2014. URL: [http://www.
757 masterflux.com/userimages/SIERRA03-0982Y3_Data_Sheet.pdf](http://www.masterflux.com/userimages/SIERRA03-0982Y3_Data_Sheet.pdf).

- 758 [43] VDI Heat Atlas, Second Edition. Springer; 2010. URL: <http://elearn.univ-ouargla.dz/2013-2014/main/document/document.php?cidReq=MEPH&action=download&id=/livreHeatAtlas.pdf>.
759
760
- 761 [44] Chang YJ, Wang CC. A generalized heat transfer correlation for louver fin geometry. *International Journal of Heat and Mass Transfer* 1997;40(3):533–44. doi:[10.1016/0017-9310\(96\)00116-0](https://doi.org/10.1016/0017-9310(96)00116-0).
762
763
- 764 [45] Kim NH, Cho JP. Air-side performance of louver-finned flat aluminum heat exchangers at a low velocity region. *Heat and Mass Transfer* 2008;44(9):1127–39. doi:[10.1007/s00231-007-0346-4](https://doi.org/10.1007/s00231-007-0346-4).
765
766
- 767 [46] Davenport CJ. Correlation for Heat Transfer and Flow Friction Characteristics of Louvered Fin. *AIChE Symp Ser* 1983;79:19–27.
768
- 769 [47] Daly S. *Automotive Air-conditioning and Climate Control Systems*. Amsterdam; Boston: Elsevier Butterworth-Heinemann; 2006. ISBN 9780750669559.
770
771
- 772 [48] Woods J. Membrane processes for heating, ventilation, and air conditioning. *Renewable and Sustainable Energy Reviews* 2014;33:290 – 304. doi:[10.1016/j.rser.2014.01.092](https://doi.org/10.1016/j.rser.2014.01.092).
773
774
- 775 [49] Zhang J, Fung AS. Experimental study and analysis of an energy recovery ventilator and the impacts of defrost cycle. *Energy and Buildings* 2015;87:265 –71. doi:[10.1016/j.enbuild.2014.11.050](https://doi.org/10.1016/j.enbuild.2014.11.050).
776
777
- 778 [50] Bilodeau S. High Performance Climate Control for Alternative Fuel Vehicle. In: *SAE Technical Paper*. SAE International; 2001,doi:[10.4271/2001-01-1719](https://doi.org/10.4271/2001-01-1719).
779
780
- 781 [51] Alahmer A. Thermal analysis of a direct evaporative cooling system enhancement with desiccant dehumidification for vehicular air conditioning. *Appl Therm Eng* 2016;98:1273–85. doi:[10.1016/j.applthermaleng.2015.12.059](https://doi.org/10.1016/j.applthermaleng.2015.12.059).
782
783
784
- 785 [52] ConsERV - Beyond fresh air. Last retrieved on March 2017. URL: <http://conserv.com/engineering/>.
786
- 787 [53] Fayazbakhsh MA, Bahrami M. Comprehensive Modeling of Vehicle Air Conditioning Loads Using Heat Balance Method. In: *SAE Technical Paper*. SAE International; 2013,doi:[10.4271/2013-01-1507](https://doi.org/10.4271/2013-01-1507).
788
789

- 790 [54] Ventilation for Acceptable Indoor Air Quality. Tech. Rep.; American
791 society of Heating, Refrigeration and Air-Conditioning Engineers,
792 inc.; 2003. URL: [https://www.ashrae.org/File%20Library/docLib/
793 Public/200418145036_347.pdf](https://www.ashrae.org/File%20Library/docLib/Public/200418145036_347.pdf).
- 794 [55] UNECE Website, Worldwide harmonized Light vehicles Test Procedure
795 (WLTP). Last retrieved on March 2017. URL: [https://www2.unece.
796 org/wiki/pages/viewpage.action?pageId=2523179](https://www2.unece.org/wiki/pages/viewpage.action?pageId=2523179).
- 797 [56] La domanda di mobilità degli italiani. Tech. Rep.; IS-
798 FORT; 2014. URL: [http://www.isfort.it/sito/statistiche/
799 Congiunturali/Annuali/RA_2014.pdf](http://www.isfort.it/sito/statistiche/Congiunturali/Annuali/RA_2014.pdf).
- 800 [57] Bütler T, Winkler H. Energy consumption of battery electric vehicles
801 (BEV). Tech. Rep.; 2013. URL: [http://oldweb.empa.ch/plugin/
802 template/empa/*/135716](http://oldweb.empa.ch/plugin/template/empa/*/135716).
- 803 [58] Wang H, Zhang X, Ouyang M. Energy consumption of electric vehicles
804 based on real-world driving patterns: A case study of Beijing. *Appl*
805 *Energy* 2015;157:710–9. doi:10.1016/j.apenergy.2015.05.057.
- 806 [59] Kelly JC, MacDonald JS, Keoleian GA. Time-dependent plug-in hybrid
807 electric vehicle charging based on national driving patterns and demo-
808 graphics. *Applied Energy* 2012;94:395–405. doi:10.1016/j.apenergy.
809 2012.02.001.
- 810 [60] Othaganont P, Assadian F, Auger D. Sensitivity analyses for cross-
811 coupled parameters in automotive powertrain optimization. *Energies*
812 2014;7(6):3733–47. doi:10.3390/en7063733.
- 813 [61] Mitsubishi i-Miev Specifications. Last retrieved December 2016. URL:
814 <http://www.mitsubishicars.com/imiev/specifications>.

815 **List of Figures**

816 1 A/C operation. In cooling mode, the system operates on a
817 refrigeration cycle. Warm air is shown entering the ERV ex-
818 changing heat first with air flowing from the cabin and then
819 with the refrigerant by means of internal heat exchangers.
820 With reference to the working fluid side, red and blue ar-
821 rows show respectively high temperature/high pressure and
822 low temperature/low pressure refrigerant. 29

823 2 Heating operation. In heating mode, the system operates on a
824 heat pump cycle. Cold air is shown entering the ERV exchang-
825 ing heat first with air flowing from the cabin and then with
826 the refrigerant by means of internal heat exchangers. With
827 reference to the working fluid side, red arrows show high tem-
828 perature/high pressure refrigerant, blue arrows indicate low
829 temperature/low pressure refrigerant. 30

830 3 ERV sensible and latent efficiencies as a function of air flow
831 rate for winter and summer operating conditions. 31

832 4 Condenser heat flux as function of air flow rate: model vs.
833 experimental data. 32

834 5 Climate variables average daily trend in Rome - winter months. 33

835 6 Climate variables average daily trend in Rome - summer months. 34

836 7 Climate variables average daily trend in different Italian cities
837 - January. 35

838 8 Climate variables average daily trend in different Italian cities
839 - July. 36

840 9 Schematic of the proposed model including the thermal block,
841 vehicle characterization and HVAC system. 37

842 10 HVAC energy consumption, expressed as a percentage of trac-
843 tion energy, for different time of commuting and month of the
844 year - Rome average summer days. 38

845 11 HVAC energy consumption, expressed as a percentage of trac-
846 tion energy, for different time of commuting and month of the
847 year - Rome average winter days. 39

848 12 Compressor electric power requirements to achieve cabin com-
849 fort in July at 13:00. 40

850 13 Comparison of HVAC energy consumption and driving range
851 values throughout summer peak day. 41

852	14	Energy savings (with reference to total energy required for	
853		traction and cabin air-conditioning) achievable employing an	
854		ERV-equipped HVAC system in summer.	42
855	15	Summer HVAC energy needs and available driving range for	
856		different Italian cities for commuting times at 8:00 (outward)	
857		and 13:00 (return). The mean value is represented with a	
858		black dot and the median with a line.	43
859	16	Summer HVAC energy needs and available driving range for	
860		different Italian cities for commuting times at 8:00 (outward)	
861		and 18:00 (return).	44
862	17	Winter HVAC energy needs and available driving range for	
863		different Italian cities for commuting times at 8:00 (outward)	
864		and 13:00 (return).	45
865	18	Winter HVAC energy needs and available driving range for	
866		different Italian cities for commuting times at 8:00 (outward)	
867		and 18:00 (return).	46
868	19	Annual energy consumption for cabin thermal comfort for a	
869		basic and an ERV-equipped HVAC system.	47
870	20	COP values for a basic and an ERV-equipped HVAC system:	
871		average values in winter months.	48

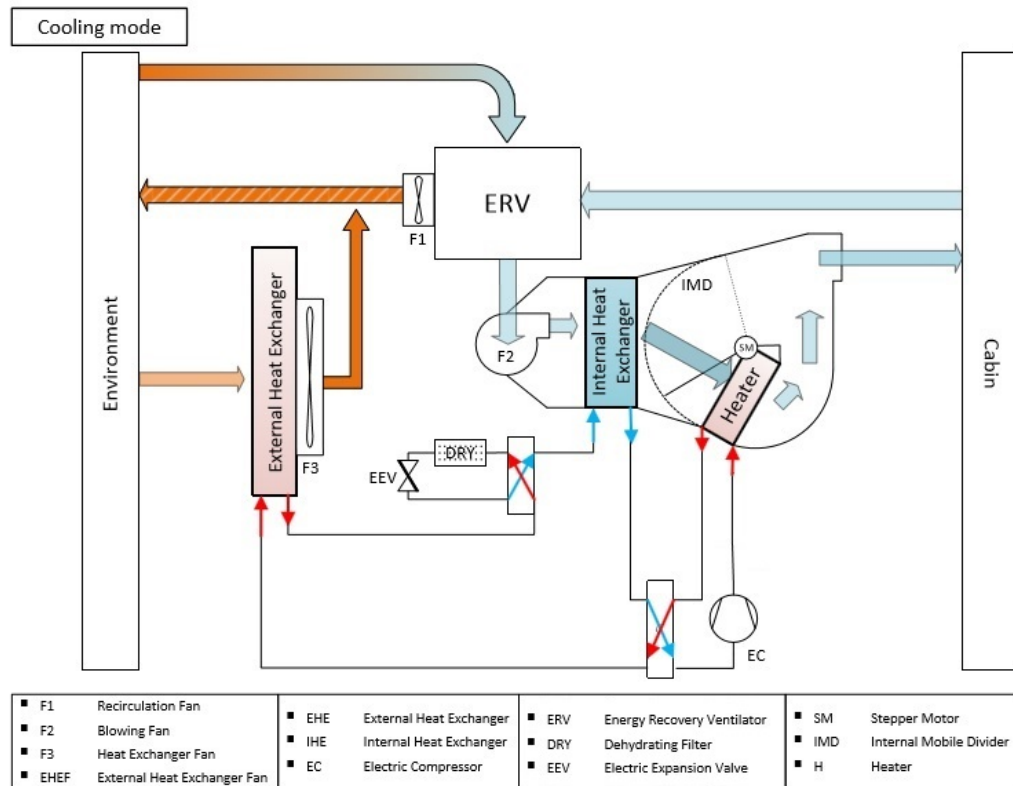


Figure 1: A/C operation. In cooling mode, the system operates on a refrigeration cycle. Warm air is shown entering the ERV exchanging heat first with air flowing from the cabin and then with the refrigerant by means of internal heat exchangers. With reference to the working fluid side, red and blue arrows show respectively high temperature/high pressure and low temperature/low pressure refrigerant.

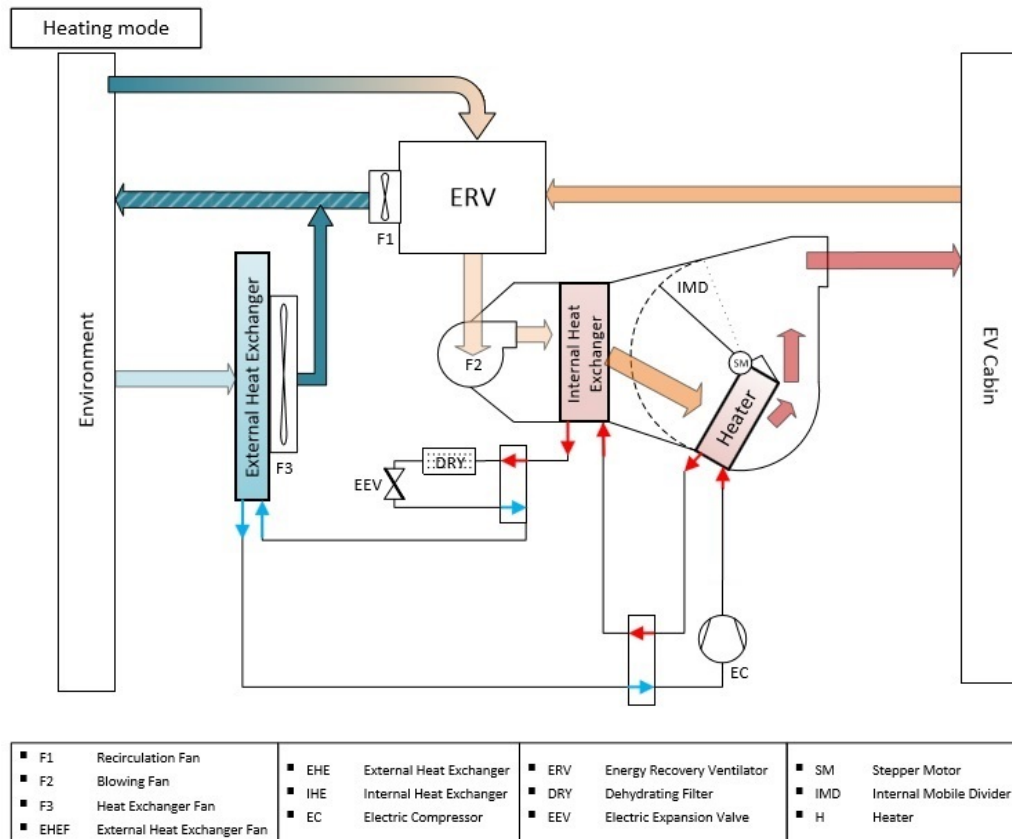


Figure 2: Heating operation. In heating mode, the system operates on a heat pump cycle. Cold air is shown entering the ERV exchanging heat first with air flowing from the cabin and then with the refrigerant by means of internal heat exchangers. With reference to the working fluid side, red arrows show high temperature/high pressure refrigerant, blue arrows indicate low temperature/low pressure refrigerant.

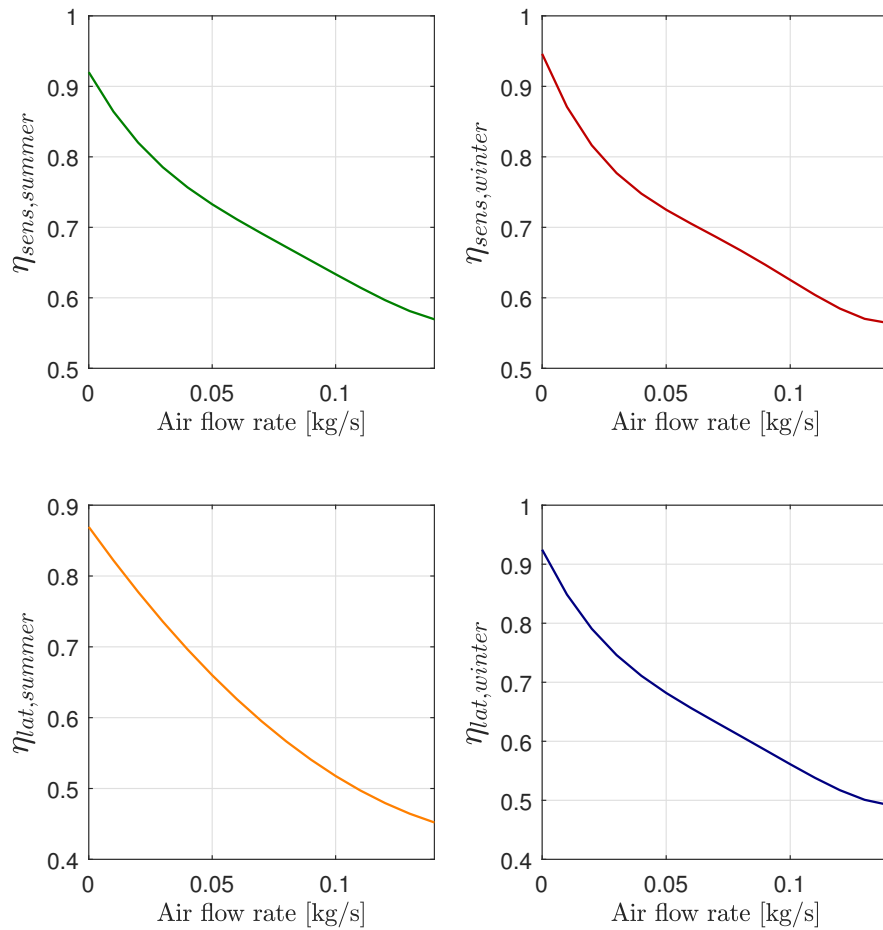


Figure 3: ERV sensible and latent efficiencies as a function of air flow rate for winter and summer operating conditions.

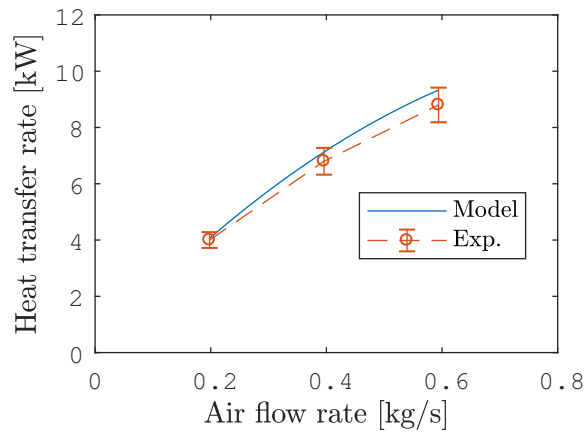


Figure 4: Condenser heat flux as function of air flow rate: model vs. experimental data.

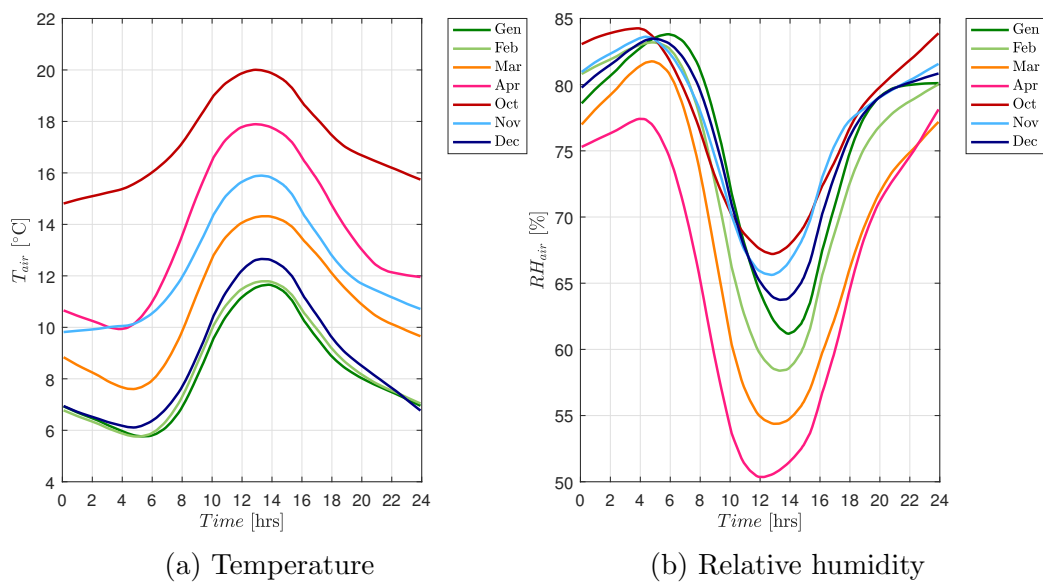


Figure 5: Climate variables average daily trend in Rome - winter months.

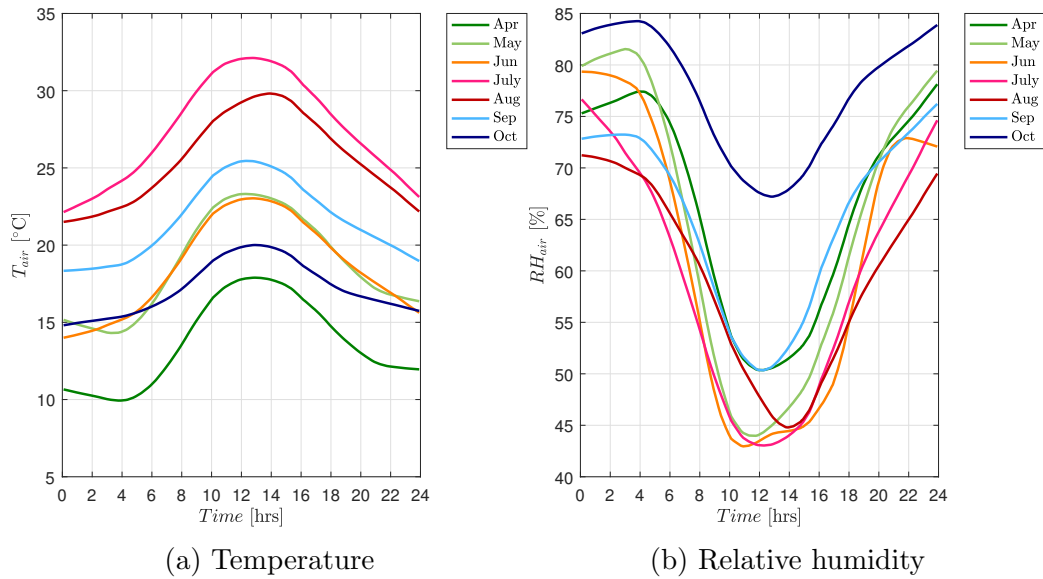


Figure 6: Climate variables average daily trend in Rome - summer months.

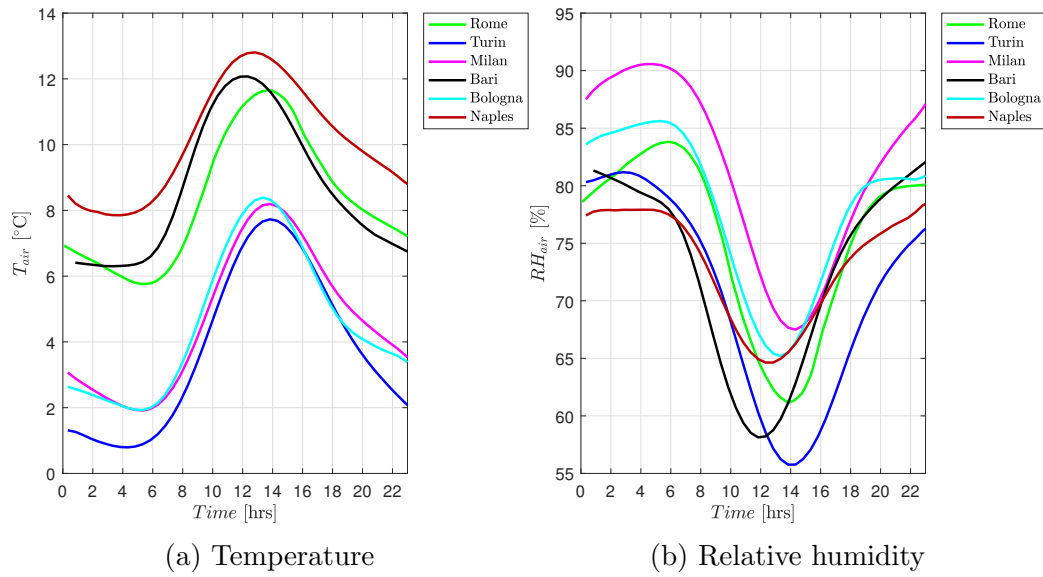


Figure 7: Climate variables average daily trend in different Italian cities - January.

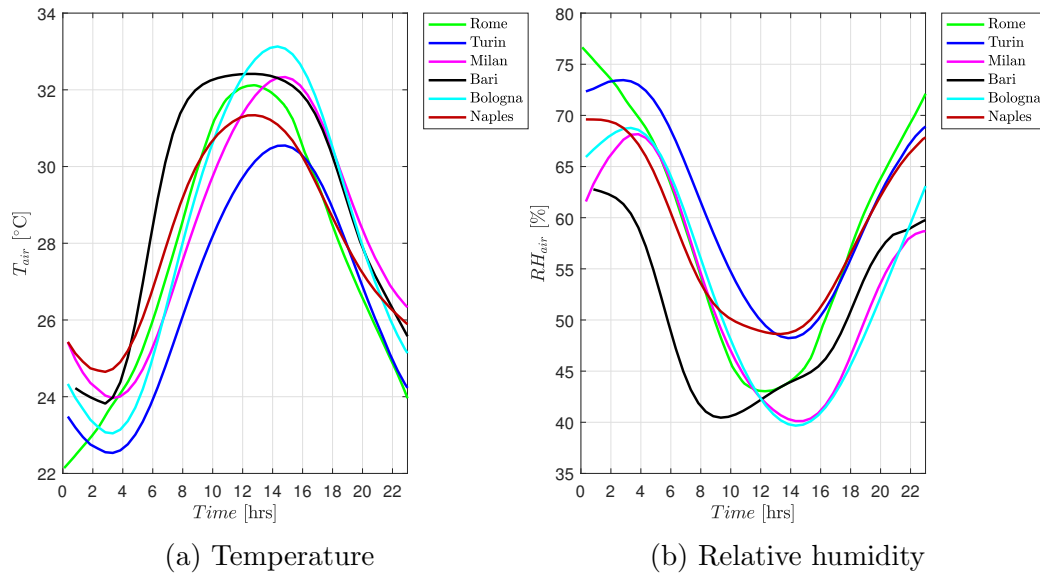


Figure 8: Climate variables average daily trend in different Italian cities - July.

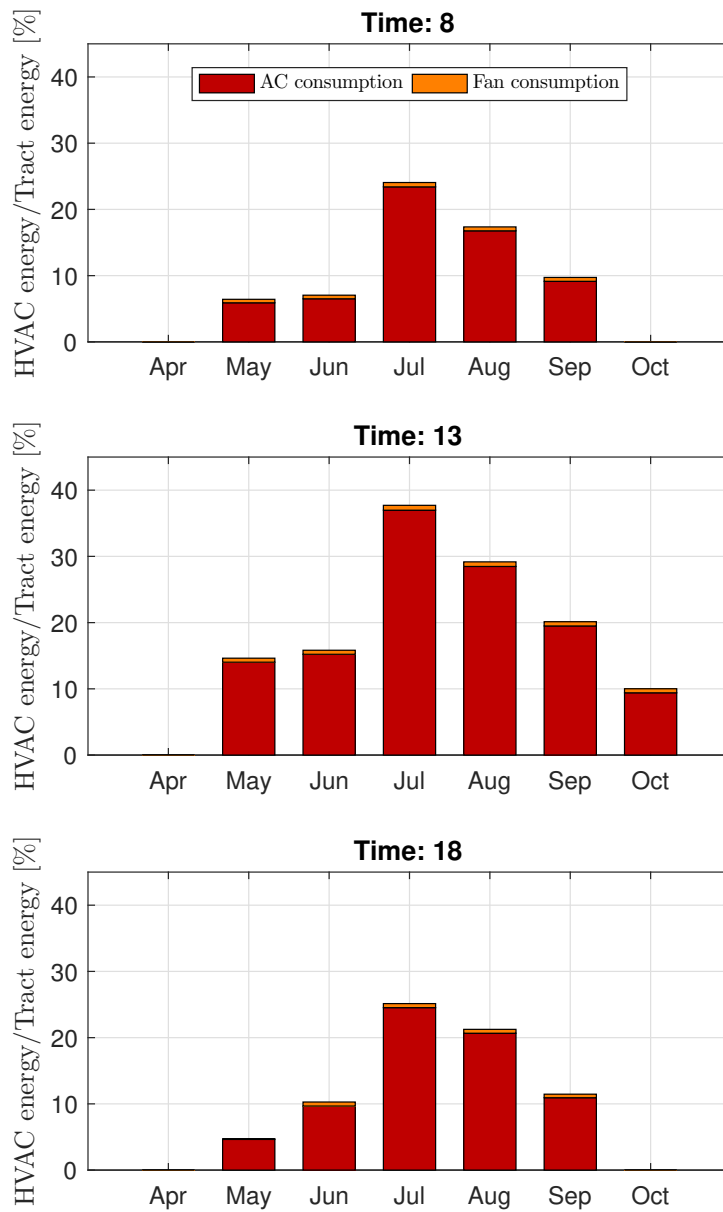


Figure 10: HVAC energy consumption, expressed as a percentage of traction energy, for different time of commuting and month of the year - Rome average summer days.

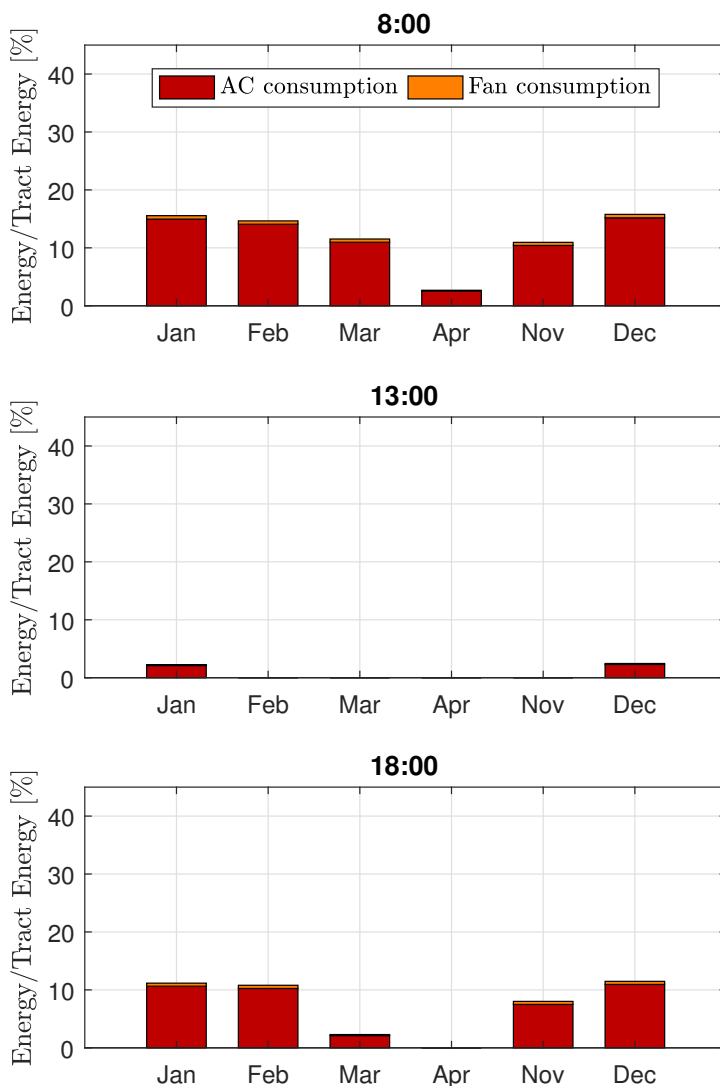


Figure 11: HVAC energy consumption, expressed as a percentage of traction energy, for different time of commuting and month of the year - Rome average winter days.

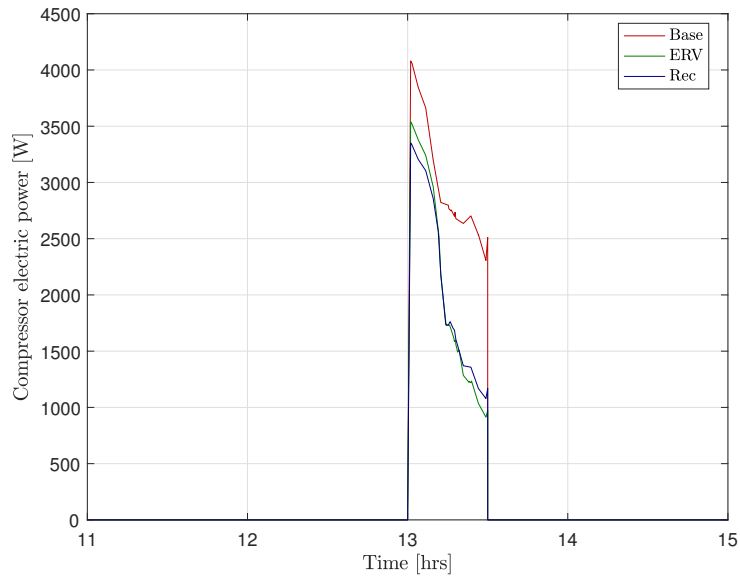


Figure 12: Compressor electric power requirements to achieve cabin comfort in July at 13:00.

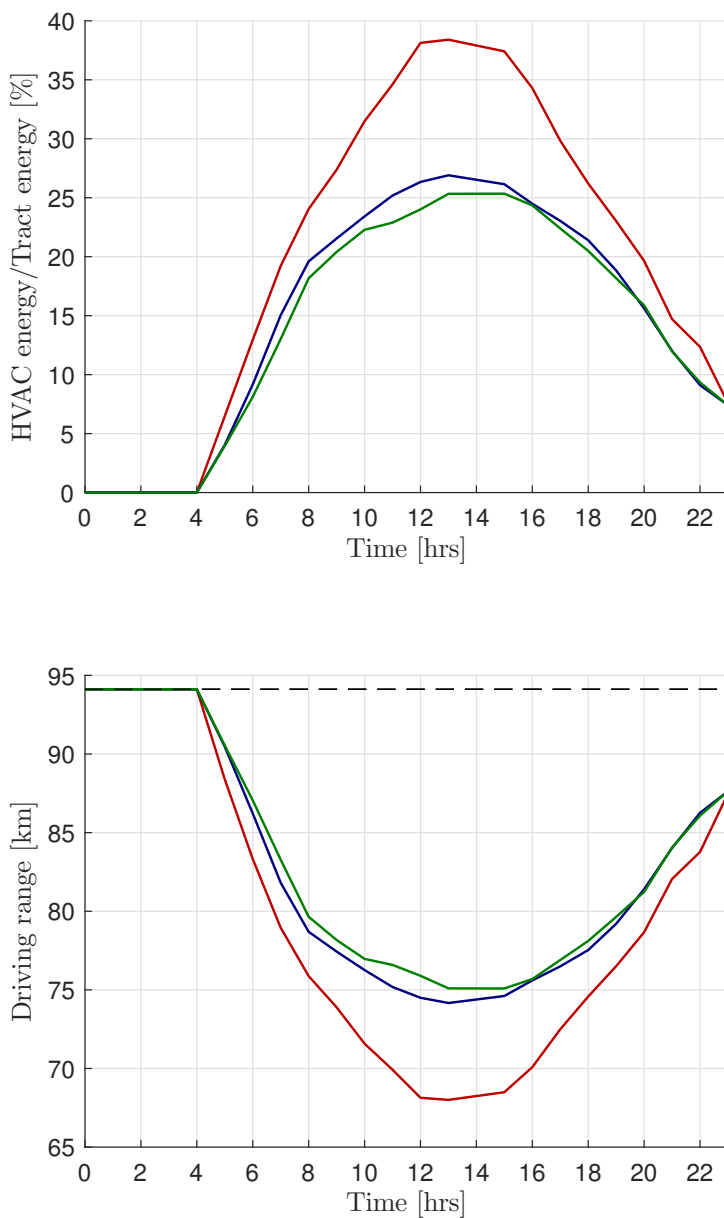


Figure 13: Comparison of HVAC energy consumption and driving range values throughout summer peak day.

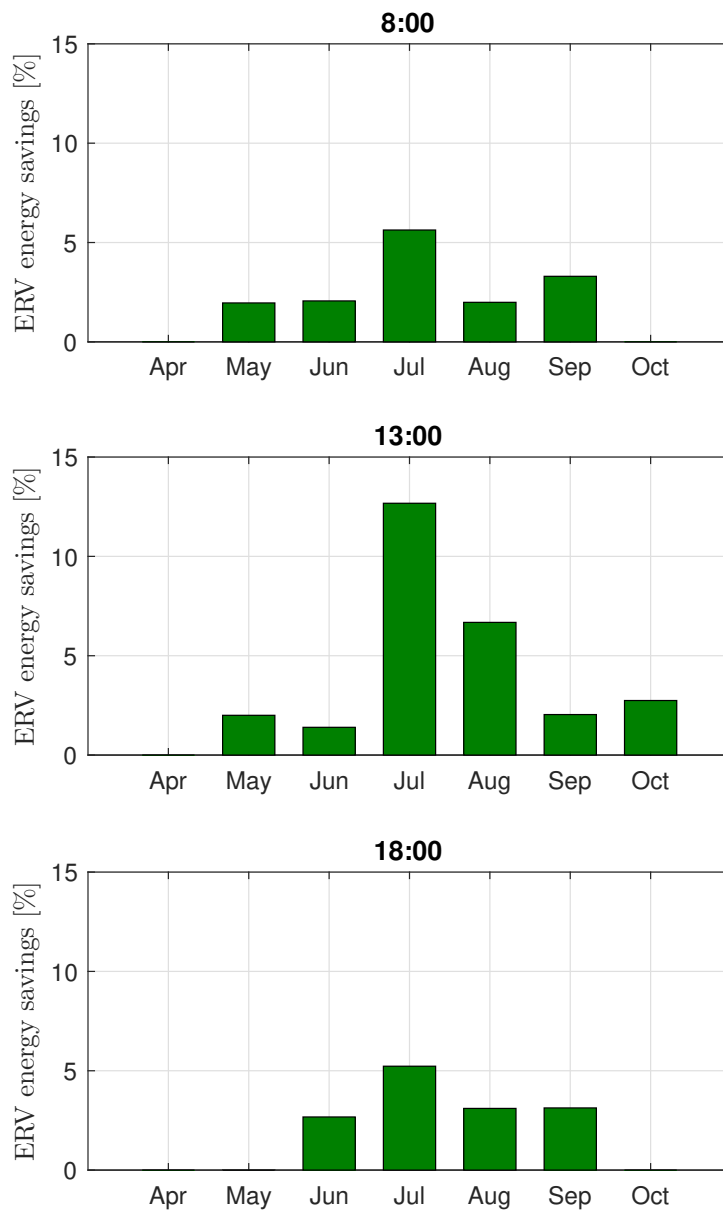


Figure 14: Energy savings (with reference to total energy required for traction and cabin air-conditioning) achievable employing an ERV-equipped HVAC system in summer.

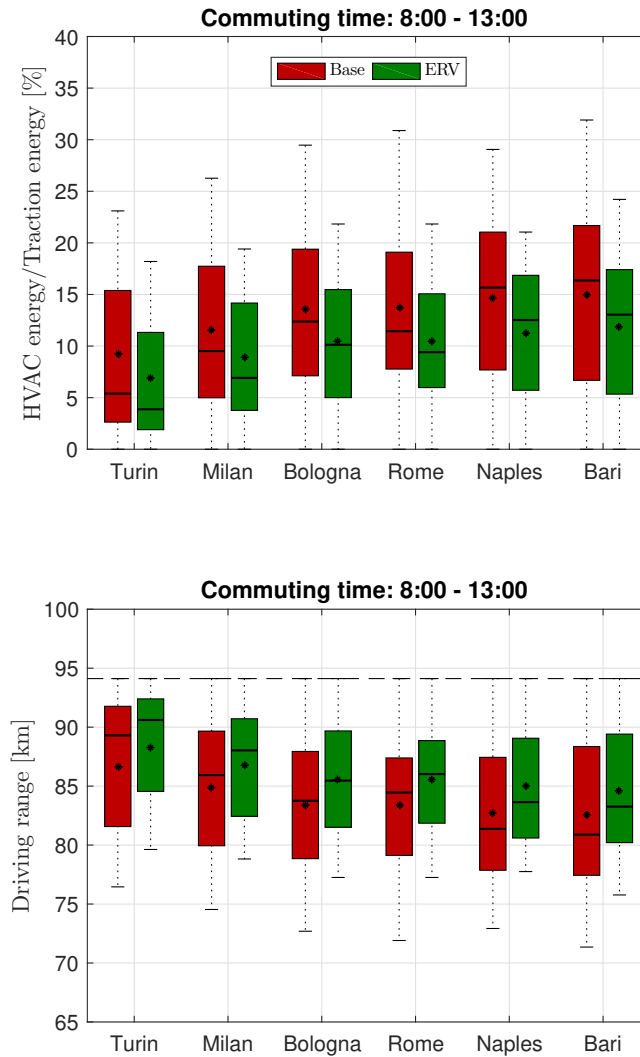


Figure 15: Summer HVAC energy needs and available driving range for different Italian cities for commuting times at 8:00 (outward) and 13:00 (return). The mean value is represented with a black dot and the median with a line.

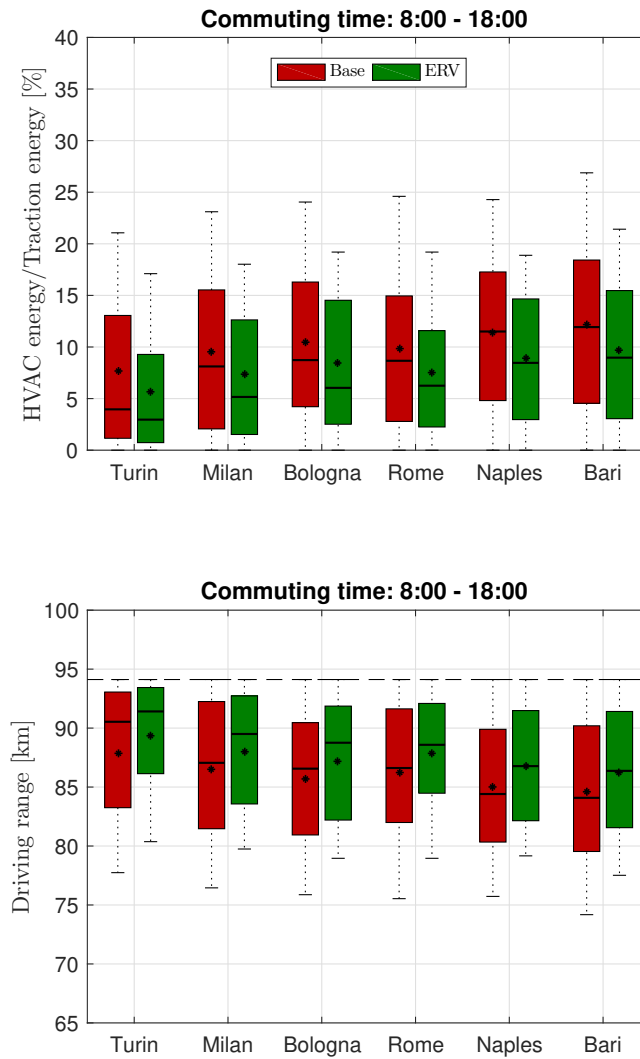


Figure 16: Summer HVAC energy needs and available driving range for different Italian cities for commuting times at 8:00 (outward) and 18:00 (return).

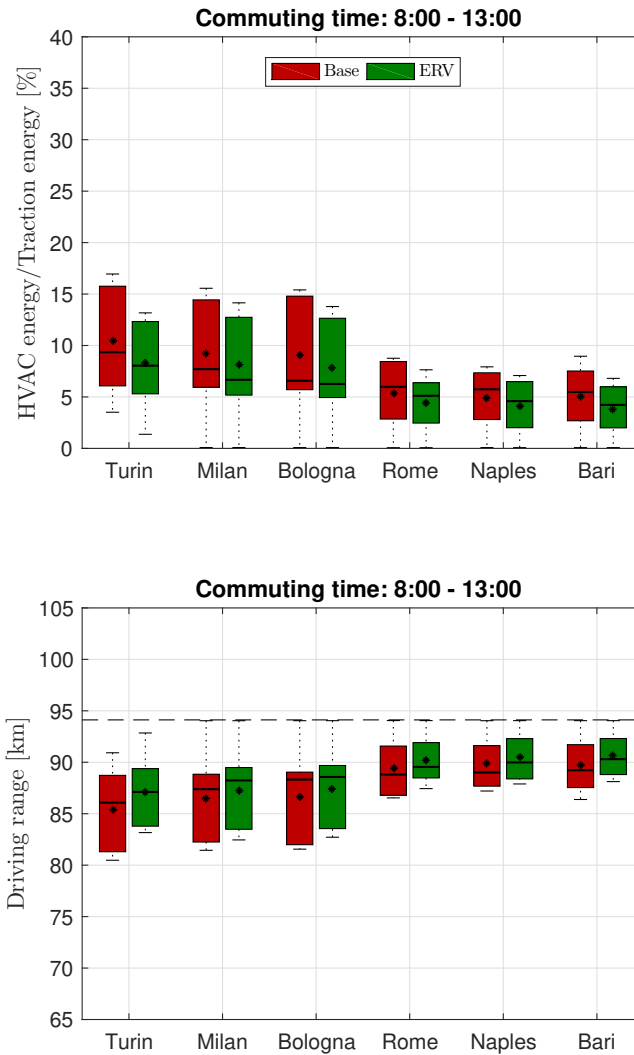


Figure 17: Winter HVAC energy needs and available driving range for different Italian cities for commuting times at 8:00 (outward) and 13:00 (return).

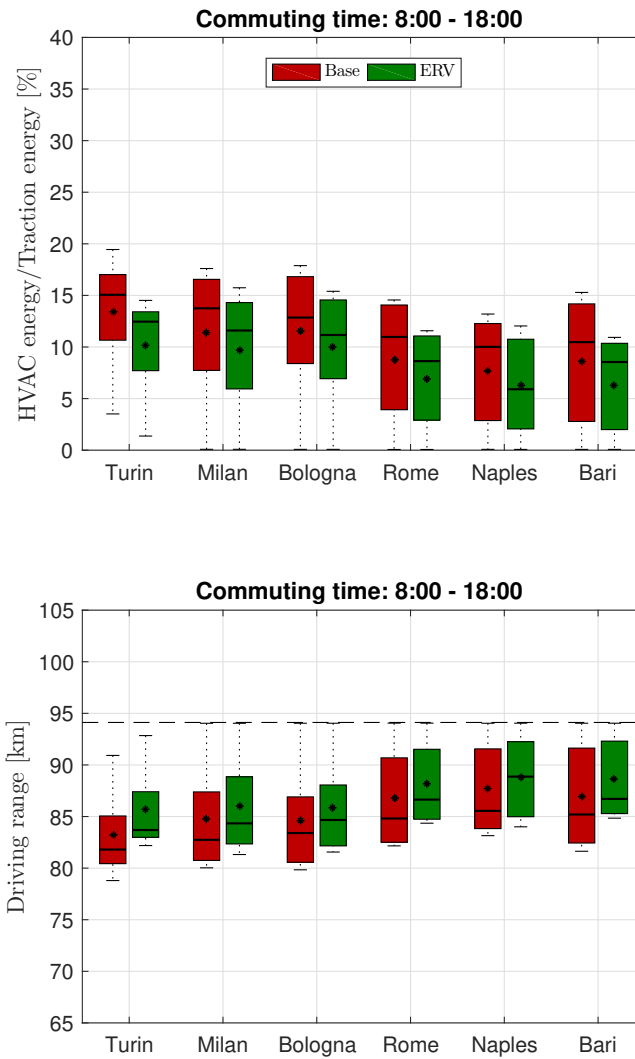


Figure 18: Winter HVAC energy needs and available driving range for different Italian cities for commuting times at 8:00 (outward) and 18:00 (return).

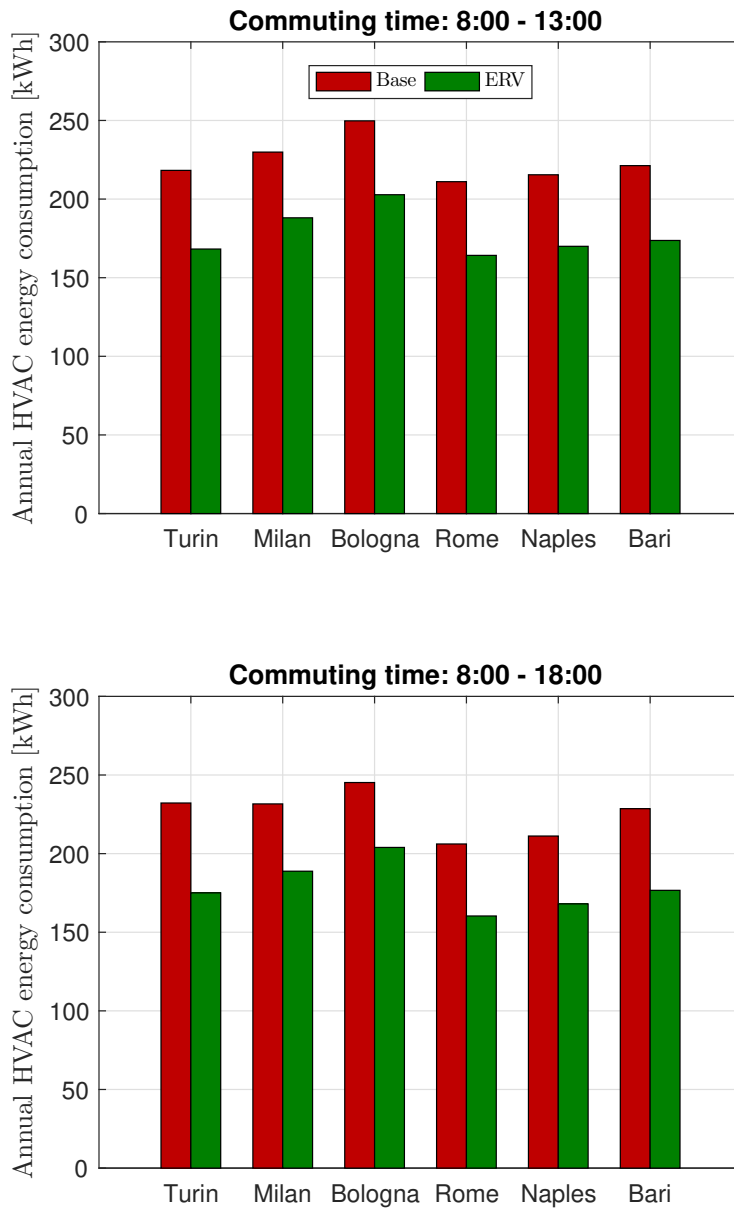


Figure 19: Annual energy consumption for cabin thermal comfort for a basic and an ERV-equipped HVAC system.

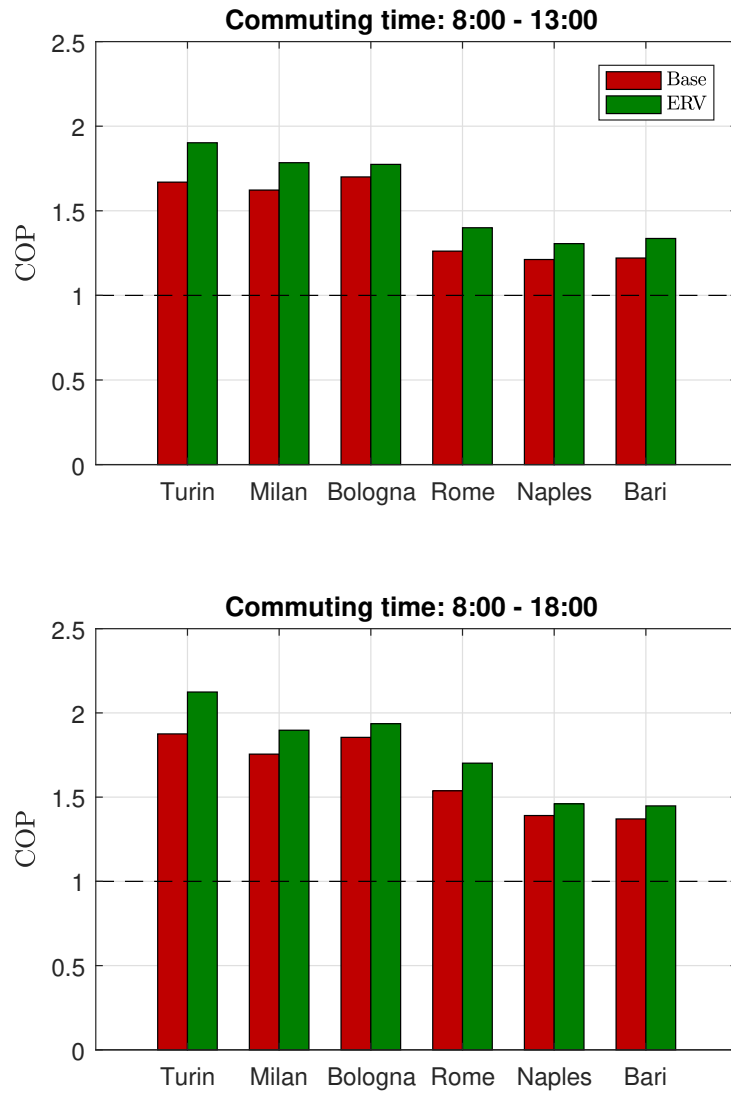


Figure 20: COP values for a basic and an ERV-equipped HVAC system: average values in winter months.